ELSEVIER

Journal of Chromatography A, 785 (1997) 135–148

JOURNAL OF CHROMATOGRAPHY A

Supercritical fluid chromatograph for studies of retention and efficiency with a brief study of *n*-alkanes showing evidence of significant temperature drop with pressure drop

Donald P. Poe*, Phillip J. Marquis[1], Tricia Tomlinson[2], Jeremy Dohm, Jie He

Department of Chemistry, University of Minnesota, Duluth, MN 55812, USA

Abstract

An instrument designed specifically to examine retention and efficiency in packed-column supercritical fluid chromatography is described. Built on a gas chromatograph, it incorporates a syringe pump, helium-actuated injector, flame ionization detector, two outlet restrictors, and direct control of column inlet and outlet pressures. A supercritical fluid solvent injection system provides chromatograms with no solvent peak or solvent-induced effects on retention and efficiency. Mass flow-rates obtained by reading the volumetric displacement at the syringe pump are accurate to within 1.4%, and the repeatability of retention times and plate numbers with the pump operated in constant pressure and constant flow modes is examined. Isopycnic plate height curves for elution of *n*-dodecane, *n*-tetradecane, *n*-hexadecane, and *n*-octadecane with carbon dioxide at 50°C and a reduced density of 1.0 on a 150×2.0-mm I.D. column packed with 10-μm Spherisorb C_8 show a broad minimum with reduced plate heights of about 2 at reduced velocities from 3 to 7, with sharp increases at higher velocities for the heavier solutes. Retention volumes decrease with pressure drop, which is attributed to a significant temperature drop from the inlet to the outlet of the column. © 1997 Elsevier Science B.V.

Keywords: Supercritical fluid chromatograph; Pressure drop; Retention behaviour; Column efficiency; *n*-Alkanes

1. Introduction

Numerous studies in recent years have shown that, at pressures and temperatures close to the critical point of the mobile phase, moderately large pressure drops in packed-column supercritical fluid chromatography (SFC) may result in significant shifts in retention [1–4] and in loss of efficiency [1,3–7]. These effects limit the ability of SFC to provide fast, efficient separations of weakly retained, thermally unstable, nonvolatile components, where the use of pure CO_2 at near-critical conditions is most desirable. In contrast, other reports have shown little or no loss of efficiency at large pressure drops [8–10]. There is currently no clear consensus on the origin or even the significance of this phenonmenon.

Studies on retention and efficiency in SFC are complicated by the complex relationships between retention, density and pressure drop. Retention is a smooth function of mobile phase density, and it has been demonstrated that, with small to moderate pressure drops, the retention factor is best represented as a function of the temporal average density [2]. One theoretical treatment of apparent plate height in SFC [7] casts the variables in the plate

*Corresponding author.

[1]Present address: Northeast Technical Services, Virginia, MN 55792, USA.

[2]Present address: Van Technologies, Duluth, MN 55804, USA.

PII S0021-9673(97)00209-4

height equation as functions of mobile phase density and mass flow-rate, and presents model plate height data in terms of isopycnic plate height curves. An isopycnic (constant density) plate height curve can be constructed by simultaneously increasing the column inlet pressure and decreasing the outlet pressure to increase the mobile phase velocity in such a fashion that the temporal average density remains constant over the entire range of velocities studied. As a result, the solute retention factors, diffusion coefficients, and other variables in the plate height equation other than velocity remain essentially constant, as in HPLC. This greatly simplifies the interpretation of an individual plate height curve, and allows for direct comparison of reduced plate height curves obtained at different mobile phase densities.

In this paper, we describe the construction and characterization of a chromatograph designed specifically to provide reliable data on retention and efficiency over a wide range of pressure drops for both unretained and retained solutes on packed-columns using supercritical carbon dioxide as mobile phase. Its major intended use, at least initially, is the generation of isopycnic plate height curves using nonpolar solutes with good chromatographic behavior. The major features of this instrument are described, with emphasis on control of mobile phase density and pressure drop, as well as on the measurement of flow-rates by several independent approaches. These features include direct control of inlet and outlet pressure, a uniform column oven temperature to ±0.2°C, and flame ionization detection of the unretained solute methane by virtue of a CO_2 solvent injection system. Aspects of instrumentation for SFC have appeared in numerous journal articles, as well as in several monographs, and all of the individual features described here have been previously reported [11,12], but have not been integrated in the present configuration and evaluated for studies on retention and efficiency. The purpose of this report is to describe the configuration of the instrument and to examine certain aspects of performance that are relevant to obtaining reliable data on retention and efficiency in packed-column SFC. A brief study using the instrument to generate isopycnic plate height curves for elution of a series of *n*-alkanes is also presented.

2. Experimental work

2.1. Overview of the SFC instrument

The overall design of the instrument is similar to one described elsewhere [13] but with significant differences in the injection system and control of the outlet pressure. The major components include an ISCO 260D syringe pump, a helium-actuated Valco CI4W injector connected to a sample reservoir, and a Varian model 2740 gas chromatograph (GC) with a flame ionization detector. This GC has a large oven that will accommodate standard HPLC-type columns up to more that 20-cm in length, as well as a large detector oven to facilitate the use of heated restrictors. The detector's electrometer was rebuilt by the Varian electronics shop with modern components. A schematic of the instrument is shown in Fig. 1.

The instrument can be operated with the pump in

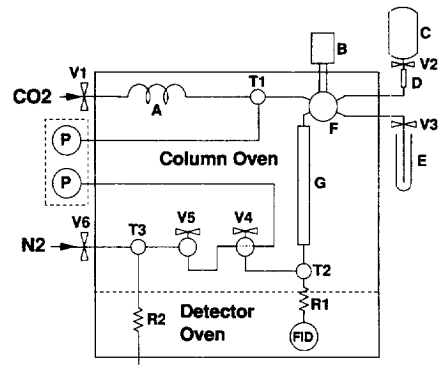

Fig. 1. Schematic diagram of the SFC instrument. V1–V6 are valves, T1–T3 are tees, R1 and R2 are restrictors. With supply valve V1 open, mobile phase flows through tempering coil A to injector F, then through column G to outlet tee T2. Some or all of the effluent flows through restrictor R1 (40-cm×30-μm I.D. fused-silica tubing) to the detector (FID). Restrictor R2 consists of 1 to 5 m of 0.005-inch (0.13-mm) or 0.007-inch (0.18-mm) I.D. stainless steel tubing, coiled in the detector oven. Valves V3–V5 are low-dead-volume valves from Valco Instruments. With valve V2 open, sample is introduced into the injector from sample reservoir C through filter D by momentarily opening valve V3, allowing excess sample to escape through restrictor E into a test tube of water. The handles of valves V4 and V5 protrude through a styrofoam lid over the sample oven. Pressure transducers P are immersed in a water bath at 25°C. Purge and vent valves (not shown), identical to V4, are inserted between the pressure transducers and T1 or V4.

either the constant pressure or constant flow mode. For operation with direct control of both inlet and outlet pressure, the syringe pump is used in the constant pressure mode to control the inlet pressure, and the outlet pressure is adjusted using compressed nitrogen. The flow-rate is then governed by the pressure drop across the column.

2.2. Syringe pump

The syringe pump reservoir is cooled to −2°C by circulating an ethylene glycol/water solution through a custom temperature-control jacket provided by the manufacturer. Thick foam insulation covers this assembly, as well as the 3.17-mm (1/8-inch) O.D. stainless steel mobile phase transfer line to the instrument, to minimize fluctuations in the apparent flow-rate due to variations in room temperature when the pump is operated in the constant pressure mode.

2.3. CO_2 solvent injector

The injection system consists of an HPLC-type injector with an internal sample loop with a volume of 60 or 500 nl, connected to a 150-ml stainless steel reservoir containing sample dissolved in CO_2 at pressures up to 90 bar. This design is similar to supercritical fluid solvent injectors described by several other workers [14,15]. This injection system is suitable for repeated injections of a test mixture, but not for routine analysis. The injector and about 1.3 m of the coiled mobile phase supply line were placed inside the column oven to equilibrate the sample and mobile phase at the column temperature. A Valco helium-driven actuator mounted outside the oven was connected to the injector with a standoff. Based on reported data [16], at 40 psi (3.7 bar absolute) helium pressure the estimated transit time of the injection rotor is less than 50 ms. Sample is introduced into the injector via 1.59-mm (1/16-inch) O.D. stainless steel tubing, connected to the sample reservoir. A low-dead-volume shut-off valve (V3 in Fig. 1) connected to the waste port is opened momentarily to fill the injection loop with fresh sample. A short length of 1.59-mm O.D. stainless steel tubing, crimped on one end, is connected to this valve with the crimped end inserted into a test tube of water. This arrangement provided visual confirmation of the sample loading operation, and minimized loss of sample. The supply valve V2 was normally left in the open position.

2.4. Column oven

A small box fan (10-cm diameter) is inserted into the column oven to provide additional air flow at temperatures up to 80°C. This provides spatially uniform temperatures to within ±0.2°C. For operation below 50°C, chilled air is blown into the oven cavity.

2.5. Column and restrictors

For operation with packed-columns with internal diameters from 1.0- to 4.6-mm I.D., the connecting tubes at the column inlet and outlet are 5 cm each of 0.18-mm I.D.×1.59-mm O.D. stainless steel. Tees T2 and T3 are low-dead-volume tees. A 5-cm length of 0.25-mm I.D.×1.59-mm O.D. tubing connects tee T2 and valve V4. This arrangement provides accurate pressure readings at the column inlet and outlet. With a 150×0.51-mm I.D. length of tubing installed in place of the column, we observed no measurable (<0.1 bar) pressure drop through the injector and connectors at flow-rates up to 1.5 ml/min liquid CO_2 at 120 bar, although it is necessary to check this after certain modifications to the system are made. In one case, after changing rotors in the injector, we observed pressure drops of up to 6 bar across the injector at high flow-rates. The rotor had not been installed exactly according to the manufacturer's specifications, resulting in poor alignment of the sample loop with the injector ports. Proper installation of the rotor alleviated this problem.

Restrictor R1, which connects tee T2 at the column outlet to the FID, is a fused-silica glass capillary, approximately 40-cm×30-μm I.D., from Polymicro Technologies (Phoenix, Arizona, USA). This linear restrictor, which should be suitable for solutes of low molecular weight, was chosen because of its simplicity and its relative freedom from plugging. Roughly 25 cm of this restrictor is located inside the detector oven at 200°C in order to maintain solutes in the gaseous state. The restrictor

was inserted into the detector through the detector's base, which had been modified to accept the restrictor through a fitting for 1.56-mm O.D. stainless steel using a graphite ferrule and stainless steel nut. The tip of the capillary was placed 25 mm below the flame tip. Restrictor R2, also in the detector oven, is one of several selectable stainless steel tubes, 0.6 to 2 m in length and 0.13- or 0.18-mm I.D., providing an outlet for fluid flows in excess of the capacity of restrictor R1.

Column outlet pressure is controlled by introducing nitrogen at tee T3. Closing either valve V4 or V5 isolates the column from the nitrogen source and secondary restrictor R2, so that all mobile phase passes to the detector. With valve V4 (a prime/purge valve) closed and valve V5 open, the nitrogen back pressure can be adjusted with the column isolated, helping to avoid undesirable pressure and flow conditions. A two-stage supply pressure regulator (410 bar maximum delivery pressure, Linde SG 3600 series, Union Carbide, Somerset, NJ, USA) was used to adjust the nitrogen pressure. Valves V3, V4 and V5 are from Valco Instruments, Houston, Texas, USA, models SFVO (V3 and V5) and SFV (V4).

2.6. Pressure transducers

Two Ashcroft (Dresser Industries, Stratford, CT, USA) model K1 pressure transducers are connected at tee T1 and valve V4 to monitor pressure at the column inlet and outlet. The transducers are partially immersed in a constant-temperature water bath at 25°C to eliminate voltage fluctuations due to changes in room temperature. The readability is ±0.07 bar and maximum hysteresis is ±1 bar. Calibration data against NIST-traceable standards were provided by the manufacturer. In order to obtain the most reliable pressure-drop data, the inlet pressure transducer was recalibrated in our laboratory against the outlet pressure transducer, using the manufacturer's data for the latter. Calibration checks, done at regular intervals, have shown no significant drift (≤0.1 bar at 100 bar) between the two units over a period of two years.

2.7. Data acquisition and detector response time

A Kipp and Zonen model BD111 analog strip chart recorder is used to record the detector signal. Full-scale pen deflection is less than 0.3 second. The recorder chart is activated by a contact closure in the Valco Digital Valve Interface unit which was also used to activate the injector. The detector time constant varies from 0.2 to 200 ms depending on the electrometer amplification factor.

2.8. General operating procedure

For generation of isopycnic plate height curves, the simplest mode of operation is to adjust the inlet and outlet pressures independently, and let the flow-rate be determined by the pressure drop across the column. With valve V4 closed, the syringe pump is adjusted to the desired pressure. Due to the relatively low flow capacity of restrictor R1, the pressure drop across the column is a few tenths of a bar, and the flow-rate is determined by restrictor R1, about 60 μl/min liquid CO_2 with the pump pressure at 120 bar. The nitrogen back pressure is then brought up to the desired value by adjusting the nitrogen regulator, and valve V4 is then opened. The flow-rate through the column is now determined by the inlet and outlet pressures and the flow resistance of the column, up to the combined flow capacity of restrictors R1 and R2. After an appropriate time for system equilibration, the injector is loaded by opening valve V3 momentarily, then actuating the injector, which also actuates the recorder.

For experiments requiring pressure drops less than about 2 bar, the pump is typically operated in the constant flow mode to avoid the possibility of reversing the flow of mobile phase through the column and to provide a more stable baseline. The outlet pressure is then adjusted with N_2. The specific combination of flow-rate and outlet pressure determines the inlet pressure and the average mobile phase density.

2.9. Experiments on elution of n-alkanes

SFC-grade carbon dioxide (no helium headspace) was obtained from Scott Specialty Gases, (Troy, MI, USA). Methane and ethane were obtained as the pure gases (99.0–99.5 mole percent) in Scotty II cylinders (Scott Specialty Gases), and propane was graded for use as a fuel in flame spectroscopy. Normal alkanes

were obtained from Alltech Associates (Deerfield, IL, USA) as a neat mixture containing equal masses of *n*-dodecane, *n*-tetradecane, *n*-hexadecane, and *n*-octadecane. The sample mixture was prepared by introducing 100 μl of the C_{12}–C_{18} alkane mixture into the sample reservoir. The reservoir was then charged with methane, ethane, and propane at 1 bar each (in addition to the air, which was not removed), followed by CO_2 at 80 bar (room temperature). The column was 150×2.0-mm I.D., packed with 10-μm Spherisorb C_8. The injection volume was 500 nl, and the detector oven temperature was at 200°C.

3. Results and discussion

3.1. Stability of flow-rate at syringe pump

Due to the compressibility of liquid CO_2 in the pump reservoir, a significant volume change occurs with a change in pump pressure, even when the liquid is cooled to −2°C. The resulting heating or cooling causes a change in the temperature of the liquid. As the liquid returns to the temperature of the cooling jacket, movement of the piston results in an apparent flow-rate reading on the pump controller display. If an experiment requires knowledge of flow-rate data at the pump, sufficient time must be allowed for thermal equilibration after adjusting the pump pressure.

In addition to the volume changes described above, syringe pumps exhibit a finite leakage rate, due to escape of fluid past the piston seal. With a good, new seal installed, we have obtained leakage rates under 1 μl/min at 120 bar and −2°C. After six months or more of the use, the leakage rates tend to increase due to wear of the seal. It has been our practice to replace the piston seal when the leakage rate exceeds 5 μl/min, approximately every 12 to 18 months.

The times required for thermal equilibration (and stabilization of pump flow) were determined following incremental pressure changes of 10 bar in the pressure range from 80 to 150 bar, with a column connected and capped off at the outlet. The time required for the apparent flow-rate to relax to the leakage rate was a minimum of 10 min, as shown in Fig. 2. For a 40-bar pressure change, the relaxation time increased to about 20 min.

3.2. Flow patterns through outlet restrictors

For pure CO_2 as the fluid at a given set of temperature conditions and restrictor geometry, and

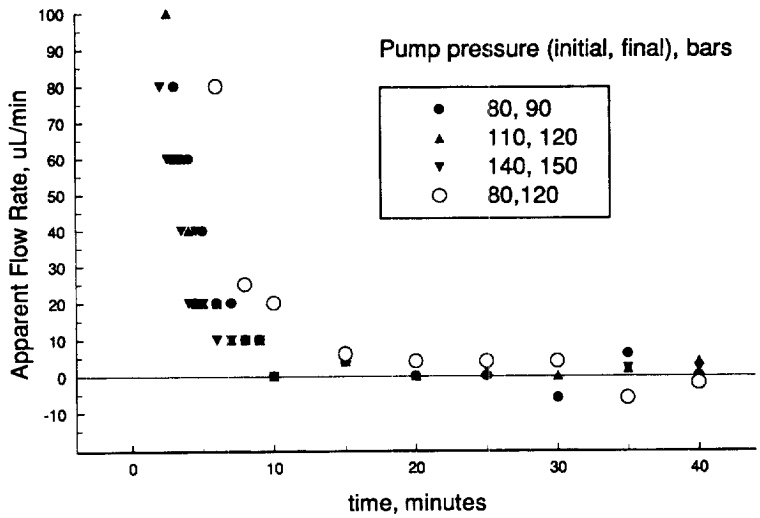

Fig. 2. Relaxation time for flow-rate after change in pump pressure. Each symbol represents the apparent flow-rate, calculated from the change in the displayed volume divided by the intervening time period, for a closed system. The time scale represents the time after a 10-bar increase in pump pressure, as given in the legend.

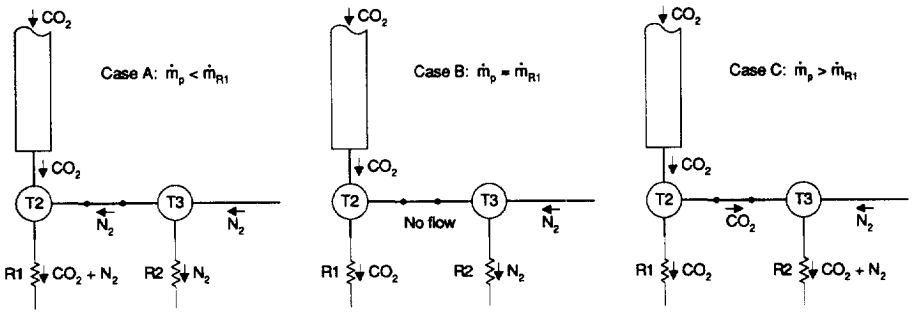

Fig. 3. Flow patterns through outlet restrictors. For each case, CO_2 is shown entering the column from the top, and N_2 is introduced on the right. Hardware items between the tees T2 and T3 are omitted for clarity. See Section 3.2 for discussion.

with the restrictor outlets at atmospheric pressure, the mass flow-rate through either restrictor R1 or R2 (Fig. 3) depends only on the outlet pressure p_o at the column outlet, which is also the inlet pressure at each restrictor. The introduction of nitrogen will affect the mass flow-rate, but it is not necessary to consider this in the qualitative analysis of the flow patterns that follows.

At a given value of p_o, let $\dot{m}_{R1}$ be the mass flow-rate of CO_2 through restrictor R1. If we let $\dot{m}_p$ represent the mass flow-rate at the syringe pump, three possible flow conditions may exist, as depicted in Fig. 3.

1. When $\dot{m}_p < \dot{m}_{R1}$, all of the column effluent and some nitrogen makeup gas will be directed through R1, so that 100 percent of an injected solute will reach the detector (Fig. 3A).
2. When $\dot{m}_p = \dot{m}_{R1}$, essentially all of the column effluent will go through R1 and all of the makeup gas through R2 (Fig. 3B).
3. When $\dot{m}_p > \dot{m}_{R1}$, some fraction of the column effluent will be diverted to R2. The maximum flow-rate, $\dot{m}_p = \dot{m}_{R1} + \dot{m}_{R2}$, is easily adjusted by selecting a tube of appropriate dimensions for R2.

For the system as described, the volumetric flow-rate at the syringe pump with R2 isolated from the system (V5 closed), and all flow directed to R1 (i.e., $\dot{m}_p = \dot{m}_{R1}$), is approximately 60 μl/min with the column oven at 50°C and $p_o = 120$ bar. This flow-rate is stable and reproducible (±1 μl/min) as long as the system is not disturbed.

Operating the unit when the column is replaced by a piece of tubing occasionally results in partial blockage of the restrictor R1 by particles sloughed off from the injector rotor. Normal flow-rates are restored by breaking off a few centimeters of the restrictor at tee T2. In a few cases when operating the unit in constant flow mode at 50 μl/min with no column present at outlet pressures below 120 bar, we have observed an oscillating baseline. This condition appears to correspond to case 2 described above, when $\dot{m}_p = \dot{m}_{R1}$. It is not surprising that the delicate balance of flows for this case would be a rather unstable condition. Because it is limited to a very small range of conditions, and we have not observed it with a column present, it does not represent a serious problem.

3.3. Comparison of flow-rates at pump and detector

Because of inherent difficulties in measuring gas flow-rates at the outlet of an operating FID, it is desirable to obtain reliable flow data at the pump. Using experimental data and the Benedict-Webb-Rubin equation of state for CO_2 [17] which exhibits an average error of 0.3% in density from 215 to 1100 K and from 0 to 3000 bar, the mass flow-rate was determined at both the pump and the restrictor outlets. For these measurements, the column was replaced with a short piece of 0.51-mm I.D. tubing, the FID was not lit, and a soap bubble meter was attached to the flame tip of the FID or to the outlet of restrictor R2. For measurements with restrictor R1 only, valve V5 was closed to prevent flow to restrictor R2. There has been some concern about the reliability of CO_2 flow-rate measurements with a bubble meter, especially at low flow-rates [18]. We

used a Hewlett–Packard (Avondale, PA, USA) model 0101-0113 soap film meter with a 100-ml capacity, with a notched cork placed on top to prevent air from flowing back into the tube, and a 2-ml latex rubber bulb filled with aqueous soap solution at the bottom. The gas flows used in this study were quite high (0.45 to 1.41 ml/s), minimizing the likelihood of errors due to absorption of CO_2 by the soap solution.

In our initial attempts to reconcile flow-rate measurements at the pump and detector, no corrections were made for pump leakage, and no special care was taken to ensure that the pump had stabilized. Measurements were taken at 6 to 9 intervals of pump pressure from 80 bar to 400 bar. With both R1 and R2 connected (R2 in this case was a piece of 45-cm×50-μm I.D. fused-silica tubing), for which the volumetric flow-rate measured at the syringe pump ranged from 0.38 to 1.82 ml/min, the average value of the ratio $\dot{m}_p/\dot{m}_{FID}$ was 1.01 (±0.03), with a maximum value of 1.05, and there was a good linear relationship between pump pressure and mass flow-rate. In this case $\dot{m}_{FID}$ represents the sum of the mass flow-rates measured at the outlets of restrictors R1 and R2. Thus at reasonably high flow-rates, the flow-rate measured at the syringe pump is quite reliable with no special precautions. However, when we repeated the experiments with only R1 connected (V4 off), the volumetric flow-rate at the syringe pump ranged from 0.06 to 0.26 ml/min, and the ratio $\dot{m}_p/\dot{m}_{FID}$ was 1.10 (±0.07), with a maximum value of 1.25 at a pump pressure of 84 bar. This demonstrates that, at low flow-rates, extra precautions are necessary to ensure reliable flow-rate measurements at the pump. With this in mind, the measurements with R1 only connected were repeated at three pressures. A minimum of 20 min elapsed after a change in pump pressure prior to taking data, and readings were corrected for leakage rate. The mass flows thus determined are listed in Table 1. In this case the average ratio $\dot{m}_p/\dot{m}_{FID}$ is 1.013 (±0.011). We conclude that, if adequate precautions are taken, reliable measurements of mass flow-rate can be based on the volumetric displacement of the syringe pump, with an uncertainty of about one percent.

3.4. Performance of CO_2 solvent injection system

Once charged and installed, the operation of the CO_2 solvent injection system is simple and straightforward. Chromatograms were obtained for solutions of methane in CO_2 and for a *n*-alkane mixture in CO_2. In both cases, the methane peak is well-formed and free from interference due to lack of a solvent peak, and the peaks for the retained solutes are also well-formed and symmetric at low to moderate pressure drops (see Fig. 4 and reference [19]). At high velocities and pressure drops, significant flattening and broadening of the peaks for the more strongly retained solutes occurs. Evidence presented in reference [19] suggests that this is probably due to temperature gradients induced by expansion of the mobile phase, and not to some characteristic of the injection system or column connections.

3.5. Repeatability of retention and efficiency data

Using the CO_2 solvent injection system and the 500-nl sample loop, sets of six injections each of methane in CO_2 were made on three successive days for each of four different operating conditions using a 2.0×150-mm I.D. column packed with 5-μm Spherisorb C_8. Data were obtained at $\langle\rho_r\rangle_t = 1.0$ and 1.5 with the pump in the constant pressure mode and in the constant flow mode. $\langle\rho_r\rangle_t$ is the temporal average reduced density [20]; $\rho_r = \rho/\rho_{cr}$, where ρ is density and ρ_{cr} is the critical density of CO_2, 0.468 g/cm^3. The results are listed in Table 2. Each row of data represents a set of six successive injections on a

Table 1
Comparison of mass flow-rates at pump and detector

Pressure (bar)	$\dot{m}_p$ (mg/s)	$\dot{m}_{FID}$ (mg/s)	$\dot{m}_p/\dot{m}_{FID}$	F_p (μl/min)	Leakage rate (μl/min)
80.0	0.7872	0.7871	1.000	48.7	0.2
120.0	1.371	1.347	1.018	84.3	0.8
120.0	1.373	1.337	1.026		
200.0	2.381	2.361	1.008	139.8	1.0

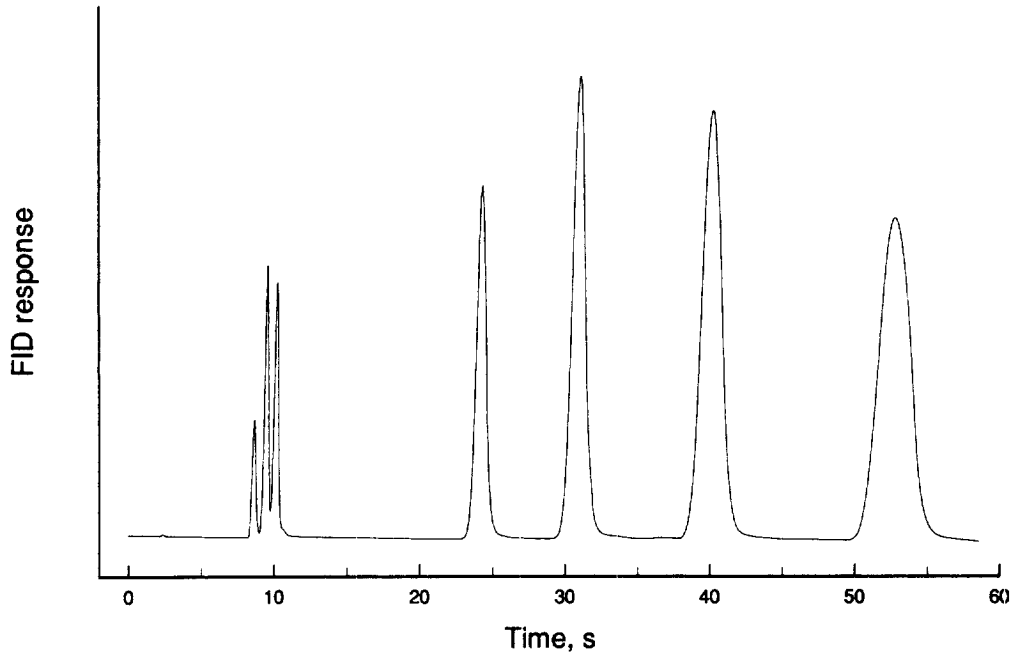

Fig. 4. Chromatogram of *n*-alkane mixture at an intermediate flow-rate and pressure drop at 50°C and $\langle \rho_r \rangle_t = 1.0$. Inlet pressure: 113.0 bar. Outlet pressure: 100.6 bar. Flow-rate at syringe pump: 1.225 ml/min of liquid CO_2 at −2.0°C. Linear velocity: 16.7 mm/s (uncorrected) or 17.5 mm/s (corrected), based on elution of methane. Column: 150×2.0-mm I.D., 10-μm Spherisorb C_8. Mobile phase: CO_2. Oven temperature: 50.2°C. Solutes: 0.50 μl of 0.067% v/v solution of a mixture containing equal masses of n-$C_{12}H_{26}$, n-$C_{14}H_{30}$, n-$C_{16}H_{34}$ and n-$C_{18}H_{38}$ in liquid CO_2, also containing methane, ethane, and propane.

single day. The average and standard deviation for retention time and plate number for each mode of operation over three days are also given. For a single set of injections on any given day, the repeatability of retention times is very good (average R.S.D.< 0.4%) regardless of the mode or average density. The day-to-day repeatability in the constant pressure mode is not so good (R.S.D.=3 to 5%), but it is quite acceptable in the constant flow mode (R.S.D.< 1%), especially at the higher density.

The larger day-to-day variations in retention time using the constant pressure mode may be due to several factors. While the readability of the pressure is 0.1 bar, setting the inlet and outlet pressures to within 0.1 bar of the desired value proved difficult, so that it was not possible to achieve the same pressure drop and flow-rate on a day-to-day basis. In addition, the measured pressure drop in the constant flow mode at 0.370 ml/min varies over a range of 0.6 bar, which is approximately equal to the hysteresis in the pressure transducers specified by the manufacturer. Finally, during these experiments the laboratory temperature exceeded 30°C, and the syringe pump had difficulty maintaining the set conditions in the constant pressure mode as indicated by significant oscillation in the piston drive rate.

Plate numbers were calculated from the peak width at half height. The repeatability of the efficiency data follows the same trends as for the retention time data, but the effects of operating mode and density are less pronounced. Again, the day-to-day repeatability is not as good as the repeatability for a single set of injections on any given day. For example, pooling all data at $\langle \rho_r \rangle_t = 1.0$ in the constant pressure mode gives an R.S.D. of 2.1% for same-day repeatability, compared to an R.S.D of 7.3% for the mean over three days. The corresponding numbers for the constant flow mode are 1.7% and 3.4%. In each case, the single-day variation reflects the uncertainty in the peak width measurement itself (±0.1 mm for a peak width of 10 to 20 mm, measure with a magnifier and reticle).

Table 2
Reproducibility of chromatographic data

$\langle\rho_r\rangle_t$	p_i (bar)	p_o (bar)	Δp (bar)	F_p (ml/min)	t_r (s)	N
Constant pressure						
1.0	110.9	102.9	8.0	0.370	27.58±0.12	6586±57
1.0	111.0	102.7	8.3	0.390	26.00±0.02	6056±213
1.0	110.9	102.7	8.2	0.380	26.78±0.17	5700±56
Mean value over three days					26.79±0.79	6114±446
1.5	155.9	144.9	11.0	0.450	31.50±0.06	7265±168
1.5	155.9	144.9	11.0	0.471	29.92±0.10	6380±132
1.5	155.9	144.9	11.0	0.471	33.13±0.13	6091±337
Mean value over three days					31.52±1.61	6579±612
Constant flow						
1.0	111.6	102.9	8.7	0.370	26.98±0.04	6465±137
1.0	111.0	102.9	8.1	0.370	27.58±0.13	6292±99
1.0	111.2	102.9	8.3	0.370	27.48±0.08	6047±60
Mean value over three days					27.35±0.32	6268±210
1.5	156.2	144.9	11.3	0.450	31.47±0.05	6228±111
1.5	156.3	144.9	11.4	0.450	31.43±0.05	6062±24
1.5	156.2	144.9	11.3	0.450	31.38±0.12	5852±134
Mean value over three days					31.43±0.05	6047±188

3.6. A brief study on retention and efficiency of n-alkanes

The instrument was used to generate isopycnic plate height curves at 50°C for elution of four normal alkanes containing even numbers of carbon atoms from 12 to 18 (*n*-dodecane through *n*-octadecane, hereafter referred to as C_{12} through C_{18}) from a 150×2.0-mm I.D. column packed with 10-μm Spherisorb C_8, using the CO_2 solvent injection system. The 10-μm packing was selected for this study to examine the performance of the system in the absence of large pressure drops near the optimum velocity. The pump was operated in the constant flow mode over the entire range of flow-rates. The sample mixture also contained methane, ethane and propane. Formally, the temporal average mobile phase density was maintained at 0.468 g/cm^3, which is equal to the critical density of carbon dioxide, or a reduced density of 1.00. Computations of density, viscosity, and temporal and spatial average quantities for pure CO_2 mobile phase were performed as described by Martire and coworkers [20,21]. The true average density in the column was probably somewhat higher than, and the average temperature somewhat lower than the specified values, as discussed later.

A representative chromatogram is shown in Fig. 4. The peaks are well formed, but the peak asymmetry ratios at half height showed a steady increase with mobile phase linear velocity, from 0.8 to 1.4 for C_{12} and 0.6 to 1.1 for C_{18}, or some degree of fronting at low velocities and tailing a higher velocities. When we replaced the column with a 150×0.13-mm I.D. stainless steel tube and injected the *n*-alkane mixture, we observed a single peak that rose very sharply, but had significant tailing with several humps on the tail, compared to a single sharp spike with little tailing for injection of methane alone. This suggests that at least some of the peak asymmetry in the chromatograms may be due to retention of solute in the linear restrictor. Replacing the linear restrictor with one of the more widely used types which have a restriction at the outlet of the capillary may result in improved peak shapes for retained solutes, especially for heavier solutes. For this study, all of the chromatograms were obtained with the linear restrictor present.

Extra-column contributions to the measured retention times and plate heights were determined by replacing the column with a 15-cm length of 0.13-mm I.D. by 1.6-mm O.D. stainless steel tubing. With the pump in constant flow mode, methane in CO_2 was injected over a range of flow-rates from 0.05 to 3.0 ml/min, and outlet pressures from 80 to 260 bar. The elution times at 110 bar fell in the range from 6.2 s at 0.05 ml/min to 0.30 s at 3.0 ml/min. The elution times at low flows were used to compute a holdup volume of 10.3 μl, including the 15 cm of added tubing. This volume was used to compute predicted elution times at high flow-rates, which were then subtracted from the measured elution times to yield an estimated lag in the response time of the detection system of 0.19 s. The extra-column holdup times as a percentage of the elution times for methane with the column present were 3.0% at 0.20 ml/min and 6.2% at 2.0 ml/min. The increased relative contribution at high flow-rates stems from the lag in response time of the detection system, which becomes significant for very short retention times.

Extra-column contributions to band variance were measured from the same set of experiments described above for extra-column holdup time. Corrections to band variance with the column present were made assuming additivity of temporal variances [22], i.e.,

$$\tau_t^2 = \tau_c^2 + \tau_{ec}^2 \quad (1)$$

where the subscripts t, c, and ec refer to total, column, and extra-column, respectively. The temporal variance was computed from $\tau_t^2 = w_h^2/5.54$, where w_h is the peak width at half height. The corrections were generally insignificant, and were greatest for weakly retained solutes at high velocities, where peak widths were most narrow. The largest correction was for C_{12} at the highest velocity, which had a retention time of 14.2 s and a peak width at half-height of 0.54 s; the extra-column variance was 4 percent of the total. For C_{18} at the same velocity, the extra-column variance was 0.3% of the total. The corrected apparent plate height is

$$\hat{H}_c = L(\tau_c^2/t_{R,c}^2) \quad (2)$$

where $t_{R,c}$ is the retention time corrected for extra-column holdup time, described above. In the discussion and figures that follow, all data have been corrected for extra-column contributions to elution time and peak variance, unless noted otherwise.

Fig. 5A shows the apparent plate heights for C_{12} and C_{18} plotted against the corrected values of linear velocity. Data at each flow-rate are the average of three successive injections. The solid symbols represent the uncorrected apparent plate height, calculated using the first expression on the right side of the equation

$$\hat{H} = L(w_h^2/5.54t_R^2) = L(\tau_t^2/t_R^2) \quad (3)$$

where L is column length and t_R is the uncorrected retention time. Because the curves swing up quite sharply at the higher velocities, especially for the heavier solutes, the data were fit to a modified version of the Knox equation

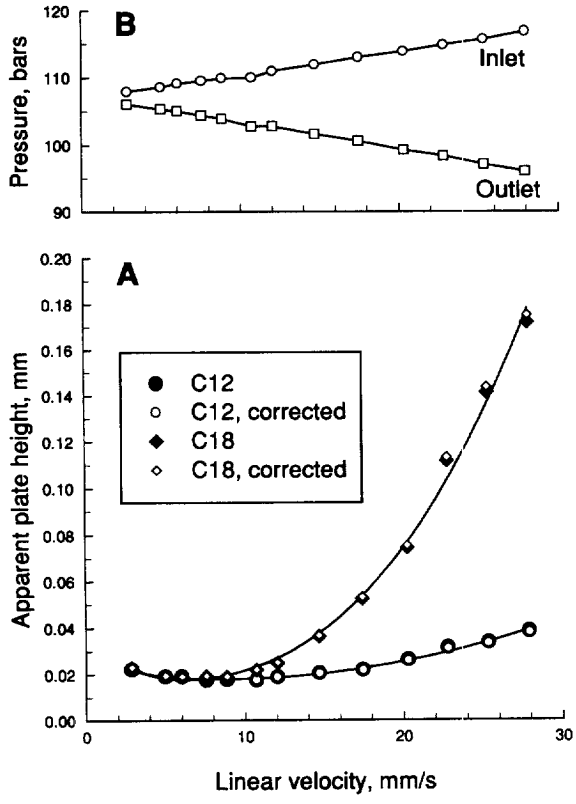

Fig. 5. Plate height curves (A) and column inlet and outlet pressures (B) for elution of four normal alkanes. Column, mobile phase, oven temperature, and solutes are the same as for Fig. 4.

$$\hat{H} = B/u + Au^{1/3} + Cu + Du^2 \quad (4)$$

where u is linear velocity. An equation of this form has been proposed [23] as an empirical fit to account for the effects of pressure drop in SFC. The smaller open symbols which overlay the solid symbols show the values of apparent plate height corrected for extra-column variance and holdup time. In general, the small negative corrections for extra-column variance and extra-column holdup time tend to balance each other, resulting in insignificant corrections to the plate height (compare Eq. (2) and Eq. (3)). Fig. 5B shows the inlet and outlet pressures used at each value of linear velocity. Given isothermal conditions at 50°C in the column, these pressure combinations should yield a temporal average reduced density of 1.00 at each velocity. The pressure drop ranged from 1.9 to 20.8 bar.

The plate height curves are plotted using reduced parameters (with the minor corrections applied for extra-column effects) in Fig. 6A. All four curves show a broad minimum with reduced plate heights of about 2 at reduced velocities from 3 to 7, which is indicative of a well-packed column and the absence of any significant contributions from extra-column effects and pressure drop in the low velocity region. Reduced apparent plate height and reduced velocity are defined as

$$\hat{h} = \hat{H}/d_p \quad (5)$$

and

$$\nu = ud_p/D_m \quad (6)$$

where d_p is particle size and D_m is the diffusion coefficient of the solute in the mobile phase. Diffusion coefficients of the n-alkanes in CO_2 were estimated using the equation of Wilke and Chang as modified for supercritical carbon dioxide [24]. Both u and D_m increase with decreasing pressure along the column axis, and strictly Eq. (6) should be written in terms of temporal average quantities. For D_m we simply used the value corresponding to the formal temporal average CO_2 density. The values of D_m computed for this study are 17.8, 16.0, 14.7 and 13.5 ($\times 10^{-9}$ m^2/s) for C_{12}, C_{14}, C_{16}, and C_{18}, respectively, at 50°C and 0.468 g/cm^3 (CO_2 viscosity = 3.48×10^{-5} Pa·s).

Fig. 6B shows the retention factors k for C_{12}–C_{18} as a function of reduced velocity, assuming methane is unretained. The k values decrease by 25–32% as the velocity is increased from the lowest to the highest value. The small increase in k for the sixth point is probably an anomaly resulting from failure to achieve precisely the desired combination of inlet and outlet pressures (Fig. 5B indicates a lower average pressure for this case, resulting in lower density and an increase in k). If the temporal average mobile phase density does not vary with the pressure drop, k should be nearly constant at lower velocities, and increase slightly at higher velocities as the pressure drop increases [7]. A possible explanation for the decrease in k is that, as the pressure drop increases, the average temperature inside the column drops due to expansion of the mobile phase. In a separate experiment, we reproduced the operating conditions with the same column present as closely

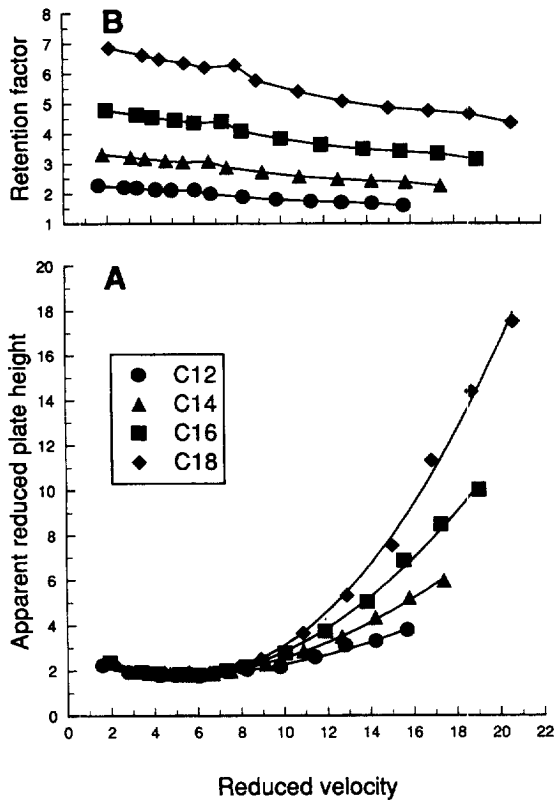

Fig. 6. Reduced plate heights (A) and retention factors (B) for elution of four normal alkanes. Column, mobile phase, oven temperature, and solutes are the same as for Fig. 4.

as possible, and measured the temperature at the column inlet and outlet by placing thermocouples on the end fittings and wrapping them with tape. The measured temperatures may not reflect the precise temperatures of the mobile phase, as no special effort was made to measure the mobile phase temperature directly. The column was used as received from the manufacturer, with a thin plastic identification label covering 60 mm of the 120-mm length between the end fittings. With no flow, the inlet and outlet temperatures were at the oven temperature of 50.3°C (compared to an oven temperature of 50.2°C for the retention and efficiency data). As the pressure drop and velocity increased, the temperature at both the column inlet and outlet decreased significantly, as shown in Fig. 7A. At the highest flow-rate, the temperature drop (difference between the inlet and outlet) was 3.8°C, and the inlet temperature was 0.6°C lower than the oven temperature. A previous study predicted that, for a column with bare stainless steel walls and operated under normal conditions with pressure drops up to 10 bar the temperature drop should be insignificant [25]. In our experiments, even at the lowest flow-rates used, the decrease in the column temperature is measurable, and the temperature drop is significant at the optimum velocity. The decrease in temperature at the column inlet may be due to failure of the mobile phase to reach thermal equilibrium prior to entering the column, or to longitudinal heat conduction in the stainless steel wall of the column. When this experiment was repeated with a 150×0.51-mm I.D. tube in place of the column, the temperature at the inlet to the tube followed the same trend as the column inlet had followed, within 0.1°C, but the temperature at the outlet fitting remained slightly higher (by 0.2°C) than the inlet. This supports the suggestion made above that some of the decrease in the column temperature with velocity may have been due to inadequate thermostatting of the mobile phase entering the column, but the rather large temperature drop along the column at large pressure drops must be due to expansion of the mobile phase. Since the average column pressure was maintained approximately constant as the pressure drop was increased, a decrease in the mobile phase temperature would result in a corresponding increase in the average mobile phase density. Because the temperature was well below the boiling points of the solutes, volatility is not a significant factor controlling retention, and an increase in density should lead to a decrease in retention. The observed decrease in retention factors with velocity is therefore consistent with the corresponding decrease in average column temperature.

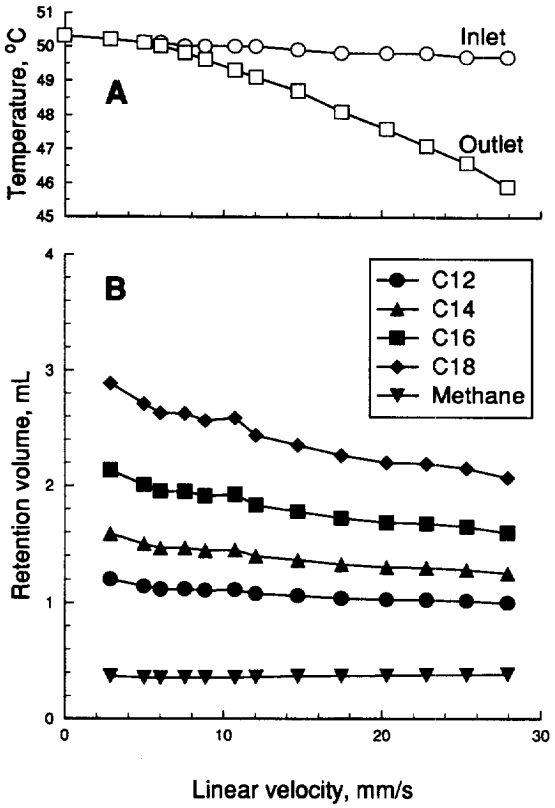

Fig. 7. Column inlet and outlet temperatures (A) and apparent retention volumes (B) of methane and the four heavier normal alkanes. Column, mobile phase, oven temperature, and solutes are the same as for Fig. 4, except that the oven temperature for A was 50.3°C.

The above explanation of the decrease in retention factors with pressure drop must be tempered by the recognition that the k values are based on the assumption that methane is unretained, which has not been demonstrated in this study. In fact, we observed three peaks for elution of methane, ethane, and propane with near baseline resolution (Fig. 4), so it is possible that methane is slightly retained. The retention time t_M of an unretained solute may be obtained by extrapolation based on the linearity of

ln$k$ versus carbon number for an homologous series in HPLC [26], but the reliability of this approach in packed-column SFC with nonuniform mobile phase conditions has not been tested. On the other hand, the extrapolation method has shown that methane is essentially unretained at temperatures and densities similar to those used in this study on an open-tubular column with SB-Octyl-50 stationary phase [18]. We decided to take the simple approach and assume that methane is unretained.

While the reliability of the k data may be questioned because they are based on the assumption that methane is unretained, the measurement of retention volumes is usually straightforward. Retention volumes were calculated as

$$V_r = F_p t_R \left(\frac{\rho_p}{\rho_{col}}\right) \quad (7)$$

where F_p is the volumetric flow-rate of liquid CO_2 at the pump, and ρ_p and ρ_{col} are the densities of CO_2 at the pressure and temperature in the pump and column, respectively. For ρ_{col}, we used the formal temporal average column density of 0.468 g/cm^3 assuming isothermal conditions at 50°C. A plot of the apparent retention volumes of methane and C_{12}–C_{18} versus linear velocity is shown in Fig. 7B. The apparent retention volumes of C_{12}–C_{18} decrease by 17 to 28 percent from the lowest to the highest velocity. It is not obvious from the figure, but the apparent retention volume of methane actually increases slightly from a minimum of 0.351 ml at 6.0 mm/s to 0.385 ml at 27.9 mm/s, a 9% increase. If methane is unretained, its retention volume must indeed be constant, and the calculated values from Eq. (7), which assumes isothermal conditions in the column and an average column density of 0.468 g/cm^3 that is invariant with pressure drop, must be incorrect. Because the column temperature does in fact decrease with increasing pressure drop and linear velocity, the assumption of isothermal conditions results in an underestimation of the actual density, leading to high results for the calculated retention volumes. The small increase in the calculated retention volume of methane with increasing mobile phase velocity is thus consistent with the corresponding decrease in the average column temperature. By similar arguments we conclude that the calculated retention volumes of C_{12}–C_{18} are also in error, and that the decrease in V_r with velocity is perhaps slightly greater than indicated in Fig. 7.

4. Conclusion

Studies on the performance characteristics of the instrument described in this paper lead to the following conclusions:

1. Accurate measurement of mass flow-rates of CO_2 from the volumetric displacement rate of the syringe pump is possible even at low flow-rates if adequate time for thermal relaxation of the pump is allowed and leakage rate is taken into account.
2. The CO_2 solvent injection system provides for chromatograms which are free from a solvent peak, which is an advantage for studies involving unretained and weakly retained solutes when using a flame ionization detector.
3. The use of a heated linear restrictor to the detector is acceptable for an unretained solute such as methane, but may cause some peak distortion even for the n-alkanes used in this study with molecular weights under 260 g/mol.
4. Repeatability of retention times is better when the pump is operated in the constant flow mode than in the constant pressure mode. The poorer repeatability in the constant pressure mode appears to be due primarily to hysteresis in the pressure transducers.

The study on retention and efficiency of n-alkanes showed that

1. the instrument can be used to generate isopycnic plate height curves with acceptable levels of extra-column holdup time and extra-column peak variance, and
2. even at moderate velocities and pressure drops with a 10-μm packing, significant temperature drops may occur in packed-column SFC, leading to increased mobile phase densities and decreased retention with increasing pressure drop.

5. Symbols

D_m	Solute diffusion coefficient in mobile phase
d_p	Particle diameter

F_p	Volumetric flow-rate at pump
$\hat{H}$; $\hat{H}_c$	Apparent plate height: uncorrected; corrected for extra-column sources
h	Reduced plate height
k	Retention factor
L	Column length
$\dot{m}_p$; $\dot{m}_{R1}$; $\dot{m}_{R2}$; $\dot{m}_{FID}$	Mass flow-rate of mobile phase: at pump; through restrictor R1; through restrictor R2; measured at FID
N	Plate number
p_i; p_o	Pressure at: column inlet; column outlet
t_R; $t_{R,c}$; t_M	Retention time: uncorrected; corrected for extra-column hold-up time; of unretained solute
u	Linear velocity of mobile phase
V_R	Retention volume
w_h	Peak width at half height
ρ; ρ_{cr}; ρ_r	Density; critical density; reduced density
ρ_{col}; ρ_p	Mobile phase density: in column; in pump
τ_c; τ_{ec}; τ_t	Temporal standard deviation from indicated source: column; extra-column; total
ν	Reduced velocity
$\langle\rangle_t$	Temporal average of quantity enclosed in brackets

Acknowledgements

Acknowledgment is made to the donors of The Petroleum Research Fund, administered by the American Chemical Society, and to the Graduate School of the University of Minnesota, for support of this research.

References

[1] P.J. Schoenmakers, L.G.M. Uunk, Chromatographia 24 (1987) 51.
[2] X. Zhang, D.E. Martire, R.G. Christensen, J. Chromatogr. 603 (1992) 193.
[3] H.-G. Janssen, H.M.J. Snijders, J.A. Rijks, C.A. Cramers, P.J. Schoenmakers, J. High Resolut. Chromatogr. 14 (1991) 438.
[4] H.-G. Janssen, H.M.J. Snijders, C.A. Cramers, P.J. Schoenmakers, J. High Resolut. Chromatogr. 15 (1992) 458.
[5] P.A. Mourier, M.H. Caude, R.H. Rosset, Chromatographia 23 (1987) 21.
[6] T.A. Berger, Chromatographia 37 (1993) 645.
[7] D.P. Poe, D.E. Martire, J. Chromatogr. 517 (1990) 3.
[8] T.A. Berger, J.F. Deye, Chromatographia 30 (1990) 57.
[9] L.M. Blumberg, J. High Resolut. Chromatogr. 16 (1993) 31.
[10] T.A. Berger, W.W. Wilson, Anal. Chem. 65 (1993) 1451.
[11] M.M. Sanagi and R.M. Smith, in Roger Smith (Editor), Supercritical Fluid Chromatography, RSC Chromatography Monographs, The Royal Society of Chemistry, London, 1988.
[12] M.L. Lee and K.E. Markides (Editors), Analytical Supercritical Fluid Chromatography and Extraction, Chomatrography Conferences, Inc., Provo, Utah, USA, 1990.
[13] M.M. Sanagi, R.M. Smith, Anal. Proc. 24 (1987) 304.
[14] W.P. Jackson, K.E. Markides, M.L. Lee, J. High Resolut. Chromatogr. Chromatogr. Commun. 9 (1986) 213.
[15] R.J. Skelton Jr., C.C. Johnson, L.T. Taylor, Chromatographia 21 (1986) 3.
[16] M.C. Harvey, S.D. Stearns, Anal. Chem. 56 (1984) 837.
[17] R.T. Jacobsen, R.J. Stewart, J. Phys. Chem. Ref. Data 2 (1973) 757.
[18] R.L. Riester, C. Yan, D.E. Martire, J. Chromatogr. 588 (1991) 289.
[19] D.P. Poe, J. Chromatogr. A, 785 (1997) 129.
[20] D.E. Martire, J. Chromatogr. 461 (1989) 165.
[21] D.E. Martire, R.L. Riester, T.J. Bruno, A. Hussam, D.P. Poe, J. Chromatogr. 545 (1991) 135.
[22] J.C. Giddings, Dynamics of Chromatography, Marcel Dekker, New York, 1965.
[23] P.A. Mourier, M.H. Caude, R.H. Rosset, Chromatographia 23 (1987) 21.
[24] P.R. Sassiat, P. Mourier, M.H. Caude, R.H. Rosset, Anal. Chem. 59 (1987) 1164.
[25] P.J. Schoenmakers, P.E. Rothfusz, F.C.C.J.G. Verhoeven, J. Chromatogr. 395 (1987) 91.
[26] G.E. Berendsen, P.J. Schoenmakers, L. de Galen, G. Vigh, Z. Varga-Puchony, J. Inczedy, J. Liq. Chromatogr. 3 (1980) 1669.